ACCOUNTS of chemical research

Article

pubs.acs.org/accounts

Accumulative Charge Separation for Solar Fuels Production: Coupling Light-Induced Single Electron Transfer to Multielectron Catalysis

Published as part of the Accounts of Chemical Research special issue "Ultrafast Excited-State Processes in Inorganic Systems".

Leif Hammarström*

Department of Chemistry, Ångström Laboratory, Uppsala University, Box 523, SE75120 Uppsala, Sweden

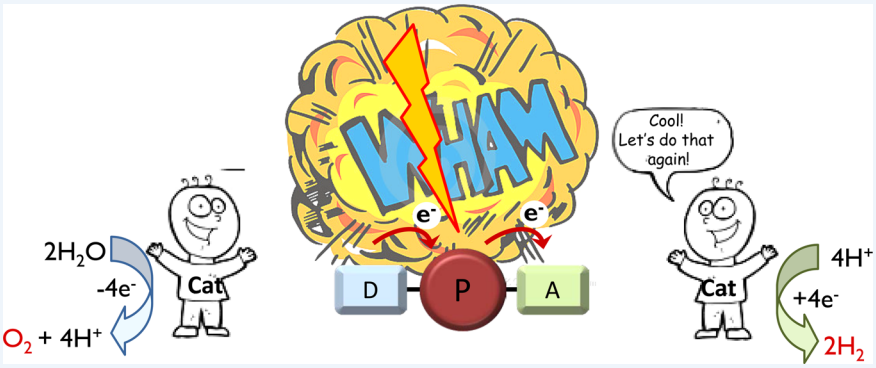

CONSPECTUS: The conversion and storage of solar energy into a fuel holds promise to provide a significant part of the future renewable energy demand of our societies. Solar energy technologies today generate heat or electricity, while the large majority of our energy is used in the form of fuels. Direct conversion of solar energy to a fuel would satisfy our needs for storable energy on a large scale. Solar fuels can be generated by absorbing light and converting its energy to chemical energy by electron transfer leading to separation of electrons and holes. The electrons are used in the catalytic reduction of a cheap substrate with low energy content into a high-energy fuel. The holes are filled by oxidation of water, which is the only electron source available for large scale solar fuel production. Absorption of a single photon typically leads to separation of a single electron−hole pair. In contrast, fuel production and water oxidation are multielectron, multiproton reactions. Therefore, a system for direct solar fuel production must be able to accumulate the electrons and holes provided by the sequential absorption of several photons in order to complete the catalytic reactions. In this Account, the process is termed *accumulative charge separation*. This is considerably more complicated than charge separation on a single electron level and needs particular attention.

Semiconductor materials and molecular dyes have for a long time been optimized for use in photovoltaic devices. Efforts are made to develop new systems for light harvesting and charge separation that are better optimized for solar fuel production than those used in the early devices presented so far. Significant progress has recently been made in the discovery and design of better homogeneous and heterogeneous catalysts for solar fuels and water oxidation. While the heterogeneous ones perform better today, molecular catalysts based on transition metal complexes offer much greater tunability of electronic and structural properties, they are typically more amenable to mechanistic analysis, and they are small and therefore require less material. Therefore, they have arguably greater potential as future efficient catalysts but must be efficiently coupled to accumulative charge separation.

This Account discusses accumulative charge separation with focus on molecular and molecule−semiconductor hybrid systems. The coupling between charge separation and catalysis involves many challenges that are often overlooked, and they are not always apparent when studying water oxidation and fuel formation as separate half-reactions with sacrificial agents. Transition metal catalysts, as well as other multielectron donors and acceptors, cycle through many different states that may quench the excited sensitizer by nonproductive pathways. Examples where this has been shown, often with ultrafast rates, are reviewed. Strategies to avoid these competing energy-loss reactions and still obtain efficient coupling of charge separation to catalysis are discussed. This includes recent examples of dye-sensitized semiconductor devices with molecular catalysts and dyes that realize complete water splitting, albeit with limited efficiency.

Received: October 20, 2014
Published: February 12, 2015

DOI: 10.1021/ar500386x
Acc. Chem. Res. 2015, 48, 840−850

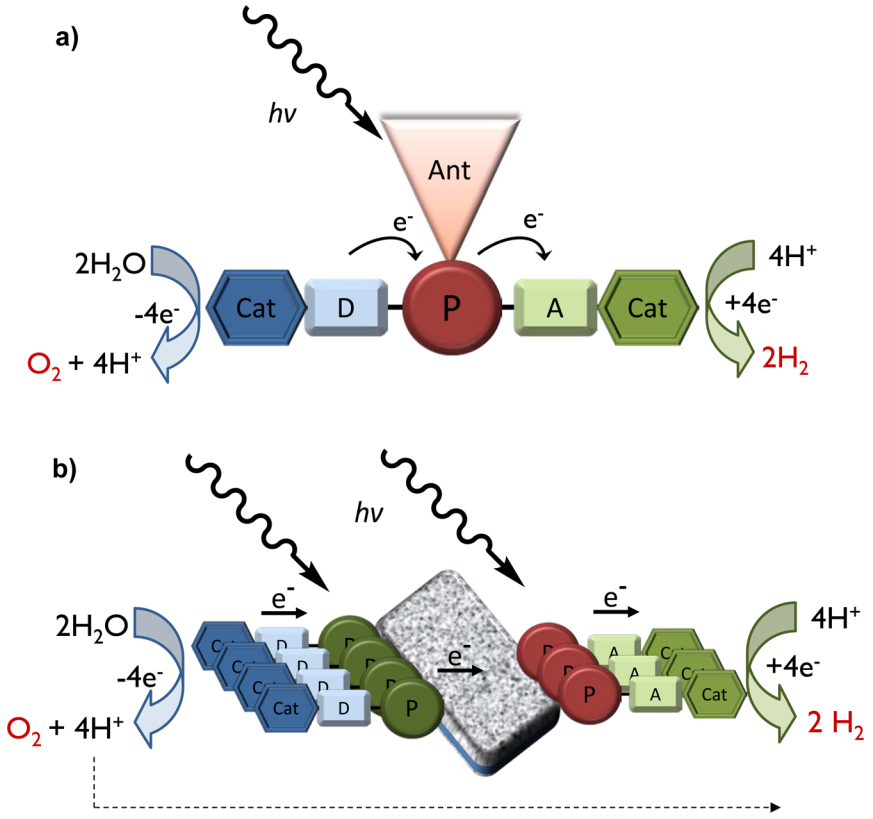

Figure 1. (a) A schematic picture of a molecular system that converts solar energy into a fuel by light-induced charge separation coupled to catalytic fuel production and water oxidation. An antenna (Ant) absorbs a photon and transfers excitation energy to the central photosensitizer (P), which transfers an electron and a hole, respectively, to the acceptor (A) and donor (D) units. The separated redox equivalents are accumulated on catalysts (Cat). On one catalyst a substrate, such as protons or carbon dioxide, is reduced to a fuel, which could be hydrogen, an alcohol, or other carbon-containing compounds. On the other catalyst, the oxidative equivalents are used to split water into molecular oxygen, thereby providing the electrons needed for the fuel production. (b) Schematic picture of a two-compartment system more loosely coupled via a "redox pool", that is, a charge transport material.

INTRODUCTION

The principles for a molecular system that converts solar energy into a fuel by light-induced charge separation coupled to catalysis have been illustrated by schemes such as that of Figure 1a.[1−3] A complete system has not yet been realized, however. Instead the different processes have been studied separately. Thus, photo-induced charge separation on a single electron level in donor−sensitizer−acceptor systems is well understood.[4] The challenge for decades of research has been to demonstrate a long-lived charge separated state with high energy that in principle can be used for chemical energy conversion.[5] Also, catalysts for water oxidation and fuel production have been developed as separate half-reactions using either electrochemical methods or addition of strong oxidants or reductants to drive the reaction.[2,6−8] Alternatively, light-driven catalysis using photosensitizers has employed sacrificial donors or acceptors to provide the complementary redox equivalents. The rational is to optimize each process separately and then couple them together. However, already the scheme of Figure 1a indicates some of the difficulties involved in their coupling. First, absorption of a photon leads to separation on the single-electron level, while the catalytic reactions require multiple redox equivalents and coupling to proton transfer reactions. There is the need to accumulate several electrons and holes, generated by the sequential absorption of several photons, before charge recombination occurs. A single chromophore absorbs at best about one photon per second under full sunlight, so an efficient light-harvesting antenna will significantly increase the chances to complete catalyst turnover before charge recombination occurs. At the same time, with a higher generation rate of redox equivalents, the catalyst would be kinetically stabilized against deleterious side reactions. Second, Figure 1a implies that the rate of water oxidation has to match that of fuel production, to balance the need for reducing equivalents. Third, there is no compartmentalization in this scheme, which means that the oxygen and fuel products are mixed, if the fuel is a gas like H_2, CO, or methane, and that oxygen may react by taking electrons from the acceptor side.

At least the last two of the difficulties above may be solved by separating the system in two half-reactions with a looser coupling via a "redox pool" (Figure 1b). This naturally allows compartmentalization and removes the requirement of matching the catalytic rate of each unit, because the ratio of oxidizing and reducing centers can be varied.

What is not immediately obvious from the schemes of Figure 1 is the specific challenges of accumulative charge separation. There are sharper energetic constraints than for single electron charge separation, because the photosensitizer must be able to oxidize and reduce the catalysts in several steps. This requires a narrow span of redox potentials for the different catalyst steps. There are also new competing and energy-wasting reactions involved that do not appear on the single electron level, as we have pointed out before.[9,10] This Account elaborates on these descriptions and gives recent examples from the literature to illustrate the principles and challenges of accumulative charge separation. It will be clear that sacrificial

DOI: 10.1021/ar500386x
Acc. Chem. Res. 2015, 48, 840−850

photocatalytic half-reactions depend entirely on the sacrificial agent to avoid competing reactions and that this is not easily replaced. Finally, design strategies will be discussed, together with examples of successful accumulative charge separation in molecular and hybrid systems, where complete water splitting into molecular oxygen and hydrogen has been achieved.

THERMODYNAMIC CONSIDERATIONS OF ACCUMULATIVE ELECTRON TRANSFER: COMPRESSING THE SPAN OF SUCCESSIVE REDOX POTENTIALS

Typical small organic molecules and symmetric dinuclear metal complexes that are able to accept or donate two successive electrons show a difference of the formal potentials for the first and second step in the range of 0.5−1.0 V.[11] This illustrates the effect of charge build-up in accumulative electron transfer. However, the potentials for successive steps cannot span a large range if accumulative electron transfer should be driven in an energy-efficient way by the oxidizing or reducing power of the same photosensitizer. By delocalization of charges on a larger molecule the successive potentials may be compressed, but at the same time, it becomes increasingly difficult to use them for coordinated multielectron catalysis. The potential difference can instead be decreased if reduction and oxidation are accompanied by structural changes. A common type of structural change is a coupled, charge compensating protonation/deprotonation. This may considerably compress the range of subsequent potentials, as exemplified by the Pourbaix diagram of $[Ru(bpy)_2(H_2O)_2]^{2+}$ (Figure 2).[12] The complex may be oxidized in four subsequent steps,

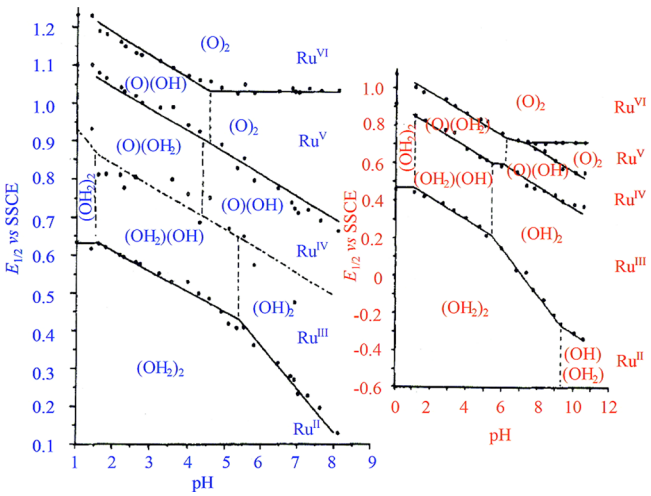

Figure 2. Pourbaix diagrams ($E'_{1/2}$ vs pH) for the water oxidation catalysts (left) *cis*- and (right) *trans*-$[Ru(bpy)_2(H_2O)_2]^{2+}$. Reproduced with permission from ref 12. Copyright 2007 American Chemical Society.

from Ru(II) to Ru(IV), within a range of only 0.6 V at a given pH, because of the coupled loss of four protons to form a dioxo complex. Proton-coupled redox steps are typical for solar fuels catalysts. For example, proton reduction catalysts react via protonation of a reduced state to form a metal-hydride intermediate.

ACCUMULATIVE ELECTRON TRANSFER AND KINETIC COMPETITION

In the construction of an efficient system for light-induced charge separation, various energetic and kinetic considerations are

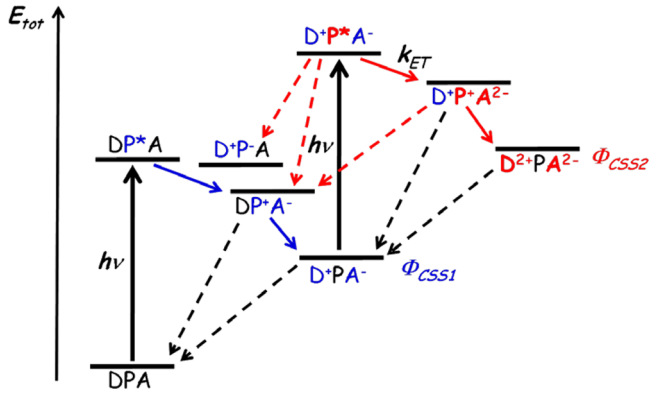

Figure 3. Reaction and state energy scheme for accumulative charge separation in a donor−photosensitizer−acceptor (D-P-A) triad undergoing successive absorption of two photons. Solid arrows represent productive reactions after the first (blue) and second (red) photon absorption; dashed arrows represent recombination reactions where red color highlights reverse electron transfers. For clarity, pathways involving initial reductive quenching of *P by D are not shown.

made. Taking a donor−photosensitizer−acceptor (D-P-A) triad as an example (Figure 3), the donor and acceptor should be chosen such that each step of charge separation leading to the D^+-P-A^- state is faster than the competing recombination reactions. Also, the excited state energies of D and A should be higher than that of P to avoid energy transfer quenching. Furthermore, D and A are often closed shell species with light atoms so that quenching by spin−spin or spin−orbit interaction is avoided.

For accumulative electron transfer, these requirements increase the difficulty of design considerably. The intermediate D^+ and A^- states are no longer closed shell species. They will also have relatively low-lying excited states, whether they are metal complexes or organic molecules, that may quench the sensitizer by energy transfer. This may happen also when these states are not observable in the D^+ and A^- absorption spectra, because exchange (Dexter) energy transfer does not require any oscillator strength for the acceptor excitation. Moreover, the excited P* is typically both a relatively strong oxidant and reductant. As is clear from the state diagram of Figure 3, there is a significant driving force for *reverse* electron transfer reactions of P* with the D^+ or A^- to reform D or A (dashed red arrows in Figure 3). This wastes the energetic state that the previous photon absorption has built up. It is important to note that the purpose of the accumulative electron transfer is to build up energetic redox equivalents for solar fuels catalysis. Therefore, the D^+ species must be rather oxidizing and the A^- reducing, so the problem of reverse electron transfer cannot be solved by changing the component energetics. Instead the system needs to be designed so that reverse electron transfer and the other energy loss reactions are slow compared with forward electron transfer that leads to accumulative charge separation.

EXAMPLES OF REVERSE ELECTRON TRANSFER

There are few studies highlighting the nonproductive reactions that compete with the accumulative process. In molecular switches based on light-induced electron transfer, it has been shown that excitation by two successive photons led to rapid reverse electron transfer, although the results were not discussed in the context of accumulative electron transfer.[13] In other cases, the second photon was absorbed by intermediate products of the

DOI: 10.1021/ar500386x
Acc. Chem. Res. 2015, 48, 840−850

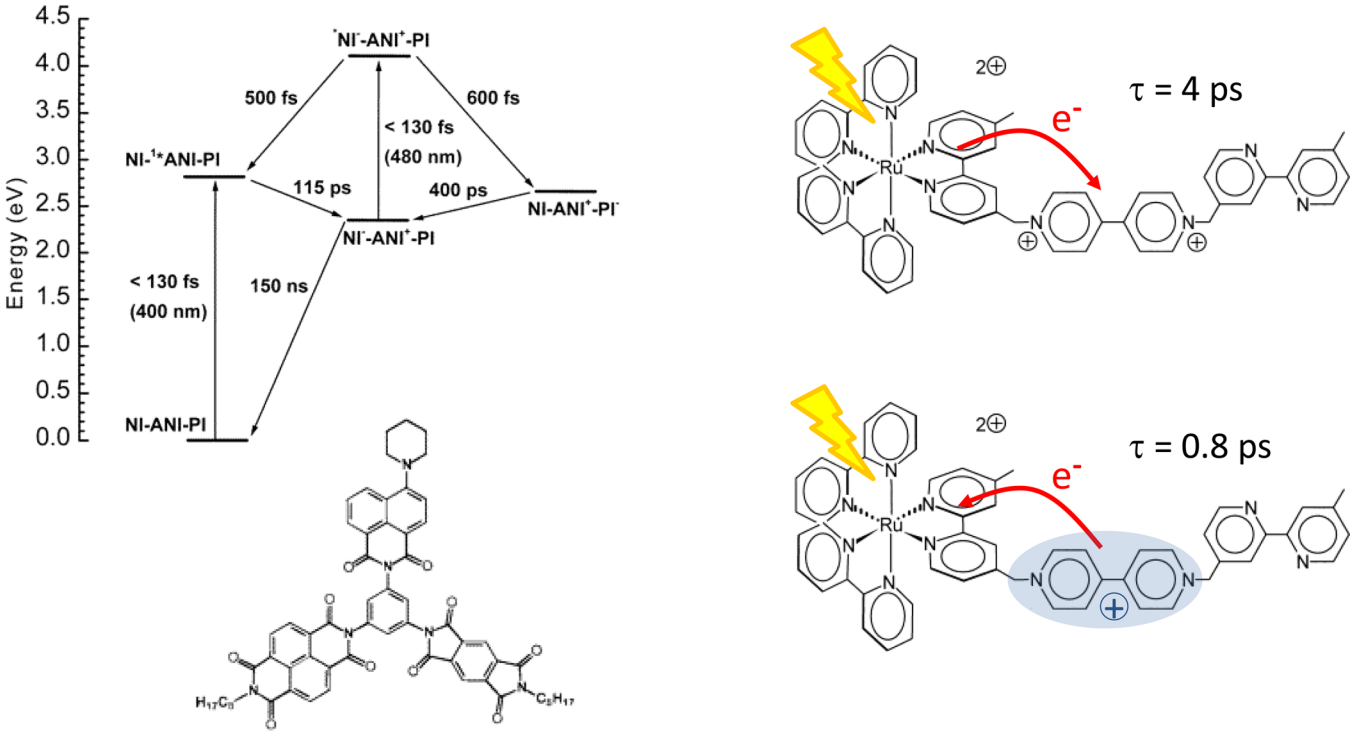

Figure 4. (left) Reaction scheme for a molecular switch where absorption of one vs two photons leads to charge transfer states with opposite directions of their dipole moments. Reproduced with permission from ref 14. Copyright 2000 American Chemical Society. (right) Switchable molecular photodiode (ref 15) where the direction of charge separation is determined by its initial redox state: $*[Ru(bpy)_3]^{2+}-MV^{2+}$ (top) or $*[Ru(bpy)_3]^{2+}-MV^{\bullet+}$ (bottom).

first electron transfer, which switched the direction of charge separation (Figure 4).[14] A third example is the reverse electron transfer shown in the dyad of $[Ru(bpy)_3]^{2+}$ (bpy = 2,2′-bipyridine) linked to methyl viologen (MV^{2+}) via a methylene group (Figure 4, right).[15] Excitation of the Ru^{2+} sensitizer in the $Ru^{2+}-MV^{2+}$ state led to the usual charge separated state $Ru^{3+}-MV^{+}$ (τ_{ET} = 4 ps). Excitation of the $Ru^{2+}-MV^{+}$ state, which was generated by electrolysis, resulted instead in rapid reverse electron transfer (τ_{ET} = 800 fs) to form $Ru^{+}-MV^{2+}$. Methyl viologen is a potential two-electron acceptor, and the reactivity of the electrogenerated $Ru^{2+}-MV^{+}$ state is a model for the first intermediate of an accumulative electron transfer. Therefore, the ultrafast reverse reaction illustrates the potential shortcomings of a system where the accumulative unit is close to the sensitizer. While the examples of this paragraph demonstrate good strategies for molecular switches, these are not useful for solar fuels production.

Compound **I** is a Ru_2-complex linked to a $[Ru(bpy)_3]^{2+}$ sensitizer at ca. 15 Å center-to-center distance.[16] The excited state reactions were examined in different oxidation states of the dimer, $Ru_2^{II,II}$, $Ru_2^{II,III}$, and $Ru_2^{III,III}$ to investigate its potential for accumulative electron transfer generating high oxidation states. However, in all states examined the excited state lifetime was quenched to <1 ns by exchange energy transfer or electron transfer *to* the Ru_2 unit. Neither of these mechanisms is productive for accumulative photo-oxidation. Because of the short excited state lifetime, **Ib** in its $Ru^{II}-Ru_2^{II,III}$ state was attached to TiO_2 nanoparticles, where ultrafast electron injection into TiO_2 could outcompete the unproductive quenching pathways and generated the photo-oxidized $TiO_2^{(-)}-Ru^{II}-Ru_2^{III,III}$. Accumulative electron transfer was not reported for this system, however.

The triad **II** was studied and excitation of the Ir-sensitizer led to the charge separation sequence $D-{}^3Ir-A \Rightarrow D^+-Ir^--A \Rightarrow D^+-Ir-A^-$ on a subnanosecond time scale and a long-lived

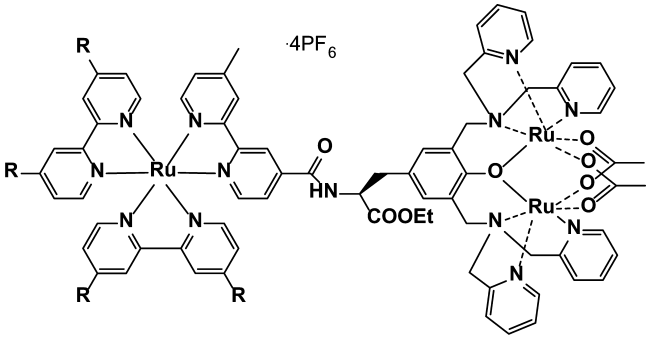

I: R=H
Ia: R=COOMe
Ib: R=COOH

D^+-Ir-A^- state (τ = 120 μs).[17] The Ir sensitizer is thus rapidly regenerated, and in experiments with 18 ns laser pulses, it may absorb more than one photon during each pulse. Yet, this did not lead to accumulative charge separation. Instead, at high laser powers a rapid decay component ($\tau \approx$ 20 ns) appeared and was attributed to reverse electron transfer from the reduced acceptor, NDI^-, in the following sequence: $D^+-{}^3Ir-A^- \Rightarrow D^+-Ir^--A \Rightarrow D^+-Ir-A^-$. Thus, the reactions after the second photoabsorption led to reformation of the same charge separated state as that formed already after one-photon absorption. This is a clear illustration of the competing reactions, in this case reverse electron transfer to the sensitizer, which may hinder accumulative electron transfer processes (cf. Figure 3).

Reverse electron transfer was also suggested by Harriman, Odobel, and co-workers for a multielectron acceptor polyoxymetallate (POM) linked to two perylenediimide (PDI)

DOI: 10.1021/ar500386x
Acc. Chem. Res. 2015, 48, 840−850

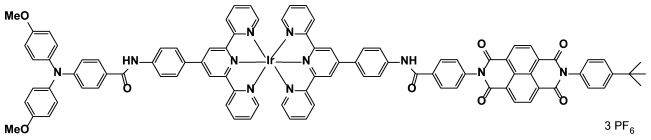

D-Ir-A

II

photosensitizers.[18] Light irradiation of PDI_2–POM in the presence of the sacrificial donor triethanol amine led to rapid buildup of the singly reduced POM^- state, but no stable further reduction was observed. Transient absorption experiments on the PDI_2–POM^- state showed a rise and decay on the 100 ps time scale, which supported the assignment to reverse electron transfer to generate PDI(PDI^-)–POM, which then returned to the same PDI_2–POM^- state as before laser excitation.

The triad of Figure 5, abbreviated $Mn_2^{II,II}$–Ru^{2+}–$(NDI)_2$, was made to model the donor side light reactions of photosystem II.[19] Excitation of the $[Ru(bpy)_3]^{2+}$-type sensitizer led to a rapid (τ = 40 ns) and unusually long-lived charge separation ($\langle\tau\rangle$ = 0.6 ms) forming the state $Mn_2^{II,III}$–Ru^{2+}–(NDI^-)(NDI) with 25% quantum yield. We noted that the $Mn_2^{II,III}$ unit could be oxidized at a potential 0.3 V below the $Ru^{3+/2+}$ potential. Also, the presence of two identical acceptor units would in principle allow a further round of charge separation, by exciting the regenerated sensitizer before the $Mn_2^{II,III}$–Ru^{2+}–(NDI^-)(NDI) state recombined and reaching the state $Mn_2^{III,III}$–Ru^{2+}–$(NDI^-)_2$ by accumulative charge separation.

We therefore undertook a study of $Mn_2^{II,II}$–Ru^{2+}–$(NDI)_2$ that turned out to illustrate several obstacles to accumulative electron transfer.[20] The sample was excited by two 10 ns laser pulses at 460 nm where one on them was delayed by 1 μs to allow the first charge separated state to form and the sensitizer to be regenerated. Each pulse converted only about 10% of the sample to the long-lived $Mn_2^{II,III}$–Ru^{2+}–(NDI^-)(NDI) state, so that 90% of the second pulse excited sample molecules for the first time. Nevertheless, the yield of reduced acceptor (NDI^-) was much smaller from the second pulse than from the first (Figure 5). Also, the initial (t = 10 ns) amplitude of the Ru^{2+} transient bleach at 450 nm and emission at 610 nm was only 90% ± 2% of the value after the first pulse. The second observation suggests that excitation of $Mn_2^{II,III}$–Ru^{2+}–(NDI^-)(NDI) led to much faster $*Ru^{2+}$ quenching (<10 ns) than in $Mn_2^{II,II}$–Ru^{2+}–$(NDI)_2$ (τ = 40 ns, see above) and that only signals from molecules excited for the first time were observed. This is corroborated by independent experiments on the corresponding Mn_2–Ru^{2+} dyad **III**: whereas the $*Ru^{2+}$ emission lifetime in the $Mn_2^{II,II}$–Ru^{2+} state was ca. 110 ns, it dropped to ca. 80 ps when the manganese unit had been oxidized to the II,III or III,III state.[21] The quenching mechanism in the $Mn_2^{II,III}$ state may be either exchange energy transfer or reverse electron transfer followed by rapid recombination. In any case the $Mn_2^{II,II}$–Ru^{2+}–$(NDI)_2$ system

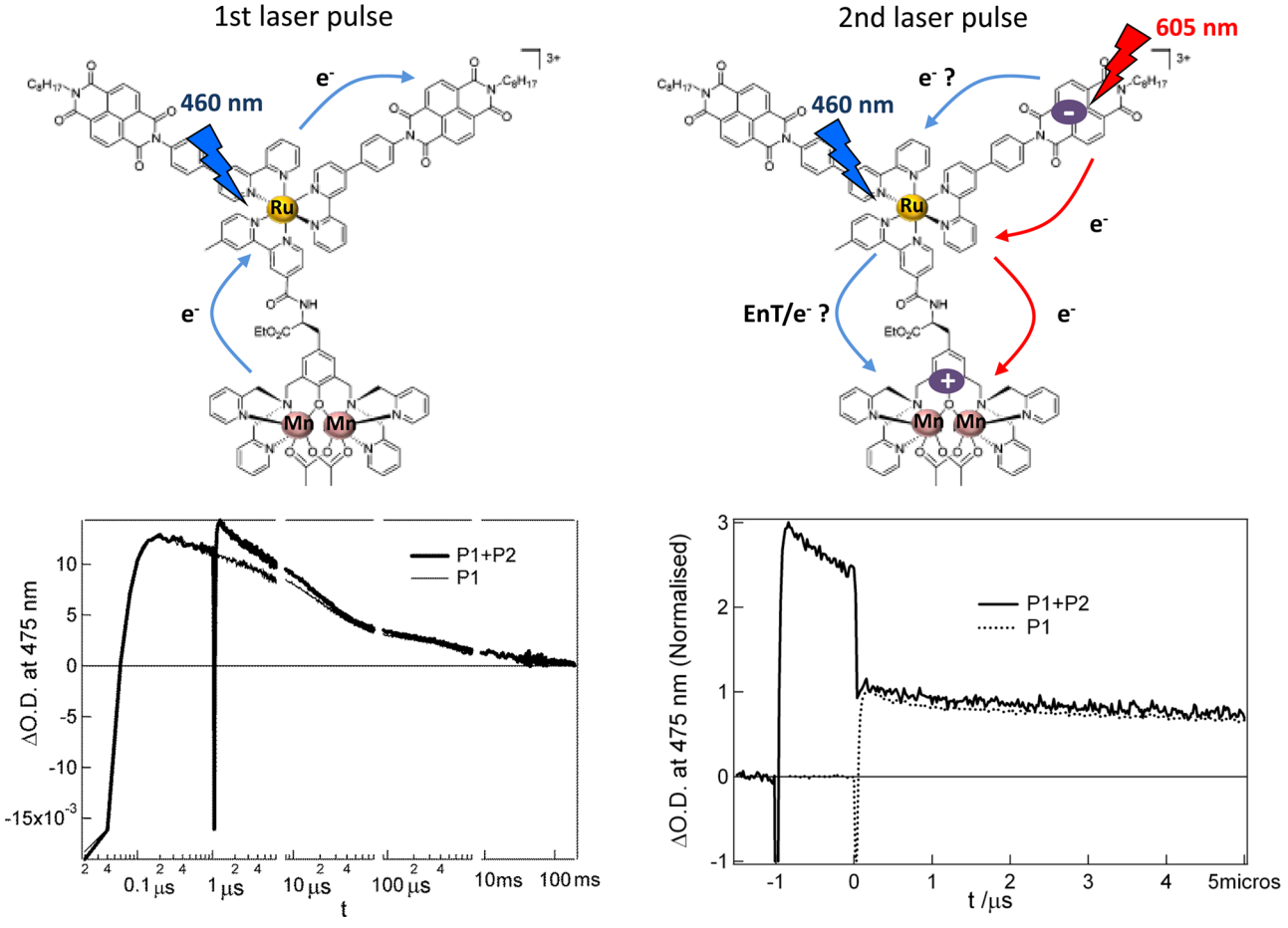

Figure 5. (top) Reaction schemes for the $Mn_2^{II,II}$-Ru^{II}–$(NDI)_2$ triad after the first and second photon absorption by the Ru unit (blue arrows) or the reduced $NDI^{\bullet-}$ acceptor (red arrows). (bottom) Transient absorption traces at the $NDI^{\bullet-}$ maximum (475 nm) after single- and double-pulse excitation at 460 nm (left) or after excitation at 460 nm (pulse 1) and 605 nm (pulse 2) (right).

DOI: 10.1021/ar500386x
Acc. Chem. Res. 2015, 48, 840–850

showed no sign of accumulative electron transfer, due to these competing reactions that were much faster (<10 ns) than electron transfer to the remaining NDI acceptor.

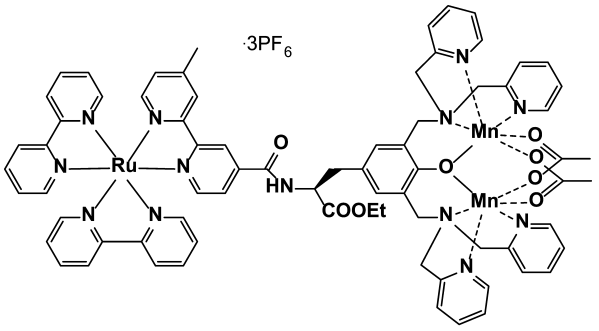

III

The first observation above, of a low $NDI^{\bullet-}$ yield in the second pulse, is related to the fact that also the $NDI^{\bullet-}$ species shows a significant absorption at 460 nm. By changing the wavelength of the second pulse to 605 nm, we selectively excited the reduced acceptor unit ($NDI^{\bullet-}$). This resulted in a substantial *decrease* of the $NDI^{\bullet-}$ signal within the laser pulse duration (<10 ns, Figure 5), without any recurrence or appearance of any new absorption features. Thus, the second pulse depleted the $NDI^{\bullet-}$ that was created by the first pulse. Because no long-lived (40 ns) Ru^{2+} emission was generated, we could exclude energy transfer as a quenching mechanism. Instead, this can be attributed to rapid electron transfer from the excited $NDI^{\bullet-}$ to the Ru^{2+} unit and further to the $Mn_2^{II,III}$ complex, thus reversing the charge separation that the first pulse had created. This illustrates also that intermediate states may absorb light and initiate unwanted processes, an effect that is related to the molecular switches above but not productive for solar fuels generation.

PHOTOCHEMICAL CATALYSIS IN SACRIFICIAL HALF-REACTIONS

Photochemical water splitting is typically initiated by oxidative quenching of the sensitizer by a sacrificial acceptor (e.g., $S_2O_8^{2-}$) that is present in high concentrations.[2,8] This ensures that the excited state is productively quenched and does not react with the catalyst in any of its oxidation states. Photochemical hydrogen production is run in a corresponding fashion with a primary reductive quenching by a sacrificial donor.[6,7] Alternatively, a one-electron acceptor is used for initial oxidative quenching, and the sacrificial donor ensures rapid regeneration of the sensitizer before charge recombination occurs. Sacrificial systems that specifically address photoaccumulation of either electrons or holes, rather than producing H_2 or O_2, follow the same principles.[22,23] In none of the above cases is the sacrificial agent easily replaced by the other half-reaction to make a complete system for reversible, accumulative charge separation coupled to catalysis. The sacrificial system is tuned to make every quenching reaction independent of the catalyst or other units that accumulate redox equivalents. The kinetics is controlled by a large concentration of the sacrificial agent compared with the catalyst, to ensure a high charge separation yield. Nevertheless, when the sensitizer is linked to the catalyst, the product quantum yield is often very low also in sacrificial systems, due to competing reactions, as discussed above for the PDI_2–POM, Ru–Ru_2, and Mn_2–Ru systems. It is therefore important to realize that while development of half-reactions with sacrificial systems may be useful to test catalysts it does not lead to development of the necessary accumulative charge separation of a complete system.

DESIGN PRINCIPLES FOR ACCUMULATIVE CHARGE SEPARATION

A solution to minimize the reactions that compete with accumulative charge separation can be summarized by the following principles. First, as described above, the excited photosensitizer can initiate several different types of reactions and is the key state where accumulative charge separation must be controlled. Therefore, the photosensitizer must be kept at a long distance from the catalysts or other multielectron donors and acceptors to slow down the competing reactions. Second, a rapid primary charge separation in the desired direction should be ensured at every step of the photocatalytic cycle by a single electron acceptor (or donor) that outcompetes other reaction pathways. Third, from this initial reaction, accumulative charge separation to the catalysts should be mediated by single-electron donors and acceptors. Fourth, a loose coupling of the oxidative and reductive half-reactions via a redox pool (Figure 1b), which is a rapid acceptor of multiple equivalents, can stabilize accumulative charge separation. The accumulated equivalents are then focused on the catalysts at each end of the half-reactions.

When these principles are used, one remaining challenge is to avoid the charge recombination reactions at each step, but this is essentially the same challenge as for charge separation on a single electron level. Another important challenge is to harvest photons at a sufficient rate to complete catalytic turnover before the accumulated charges recombine.

Photosystem II illustrates these principles very well (Figure 6).[24,25] The primary electron transfer from the excited chlorophylls ($*P_{680}$) to the pheophytin occurs with $\tau \approx 3$ ps. This is followed by further single-electron transfer steps to generate Q_A^- and $Tyr_Z^{\bullet}$. These species then react with the multielectron acceptor (Q_B) and donor (the water oxidizing $CaMn_4$ complex) that are kept at some distance from the central chlorophylls (ca. 22 and 13 Å edge-to-edge, respectively). Nevertheless, even at 13 Å distance, quenching reactions could potentially occur on the sub-nanosecond time scale, as illustrated by the reactions of **I** and the triad of Figure 5 above where the center-to-center distance is ca. 15 Å. Therefore, the high rate of electron transfer to the pheophytin is presumably needed to obtain a high charge separation yield also in the later stages of the water oxidation photocycle. Figure 6b illustrates that the driving force is large for the $*P_{680}$ to react by reverse electron transfer from Q_B^- and to the $CaMn_4$ complex in its higher oxidation states. Finally, the thylakoid membranes of oxygenic photosynthesis follow the loose coupling of Figure 1b, as several copies of photosystems I and II are coupled via reducing equivalents of the plastoquinone pool and electron transfer proteins, instead of being coupled directly one-to-one.

EXAMPLES OF ACCUMULATIVE ELECTRON TRANSFER IN MOLECULAR/SEMICONDUCTOR HYBRID SYSTEMS

The first example of a molecular system for accumulative charge separation with a regenerative photosensitizer was realized taking the above principles into account (Figure 7).[26,27] The oligotriarylamine (OTA) donor can be oxidized twice at a potential below that for the $Ru^{II/III}$ couple, and the visible absorption of the resulting OTA^+ and OTA^{2+} species are strong and distinctly different. In analogy to dye-sensitized solar cells

DOI: 10.1021/ar500386x
Acc. Chem. Res. 2015, 48, 840–850

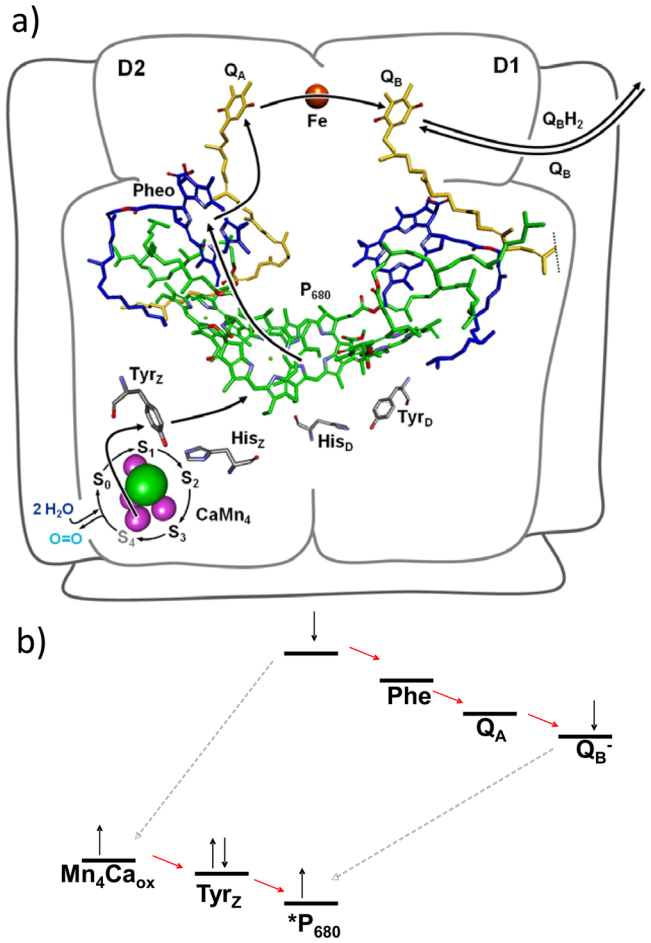

Figure 6. (top) Structure of the redox cofactors of photosystem II; electron transfer reactions are indicated by arrows. Reproduced with permission from ref 24. Copyright 2011 Royal Society of Chemistry. (bottom) A qualitative frontier orbital energy diagram for charge separation (red arrows) emphasizing the potential for reverse electron transfer reaction (dashed arrows) when Q_B is reduced and the $CaMn_4$ cluster is oxidized. This does not correctly describe the electronic structure of $^*P_{680}$ and $CaMn_4$ but illustrates the redox reaction energetics.

(DSSCs), the excited Ru^{II} sensitizer rapidly (<1 ps) injected electrons into the mesoporous TiO_2 film, which can accept many electrons per particle. The Ru^{III} species oxidized the OTA within 1 ns to result in the $TiO_2{}^{(-)}$–Ru^{II}–OTA^+ state in 100% yield, as estimated from the relative extinction coefficients. This state recombined with typical multiphasic kinetics typical for dye–TiO_2 systems, on the time scale of 10–1000 μs. In double-pulse experiments, a second 10 ns excitation pulse was applied 1 μs after the first, when the sensitizer was regenerated but before significant recombination had occurred. Each laser pulse excited 30% of the sample so that 70% of the second excitation was in molecules that were excited for the first time. Nevertheless, the resulting transient spectrum was distinctly different from that after single excitation (Figure 7). After subtraction of the 70% single excitation product, the spectrum was in excellent agreement with the reference spectrum for the doubly oxidized donor OTA^{2+}. The absorption magnitude showed that ca. 100% of the sample that was excited by two pulses (30% × 30% = 9%) had been converted to the $TiO_2{}^{(2-)}$–Ru^{II}–OTA^{2+} state, that is, the yield of accumulative charge separation was as high as 100%. This state showed the same relatively slow recombination kinetics as that after the first excitation pulse, because recombination is determined by the intrinsic properties of the TiO_2 film.[28]

The significance of this result is that it was the first proof-of-principle experiment showing accumulative charge separation in a molecular system with a regenerative sensitizer and a multi-electron donor. This was a reversible reaction that transiently stored free energy, in contrast to sacrificial systems. It did so on a time scale up to 1 ms, which is similar to the time scale of catalytic turnover in, for example, photosystem II (ca. 500 s^{-1}) and hydrogenase enzymes (up to 1 × 10^4 s^{-1}).[25] This shows the possibility to replace the OTA with a catalyst and develop systems for accumulative charge separation coupled to solar fuels catalysis. Under solar irradiation conditions, an antenna function with many light-harvesting dyes would be required to provide redox equivalents to the catalysts at a rate compatible with such large turnover rates. Nevertheless the laser studies show that accumulative charge separation on a time scale relevant for molecular catalysis is feasible. The success of the system depended on the principles outlined above and the slow recombination in sensitized TiO_2 systems.

Recent studies by T. J. Meyer and co-workers extended the concept by using potential water oxidizing Ru(II) catalyst complexes as donors. With **IV** attached to TiO_2 films, laser flash excitation led to rapid (<20 ns) electron injection into TiO_2 and oxidation of the catalyst to form $TiO_2{}^{(-)}$–Ru_a^{II}–Ru_b^{III}.[29] The quantum yield was only 10%, because the lowest excited state is localized on Ru_b^{II}. This has a short intrinsic lifetime (<20 ns) and is not directly attached to TiO_2, which presumably made electron injection slow. When **IV** was electrochemically preoxidized to TiO_2–Ru_a^{II}–Ru_b^{III} the laser flash excited primarily Ru_a^{II} states, which led to formation of $TiO_2{}^{(-)}$–Ru_a^{II}–Ru_b^{IV}=O in <20 ns and in 15% yield. A reasonable assumption is that the low yield is due to excited state electron or energy transfer to the Ru_b^{III} unit competing with electron injection.

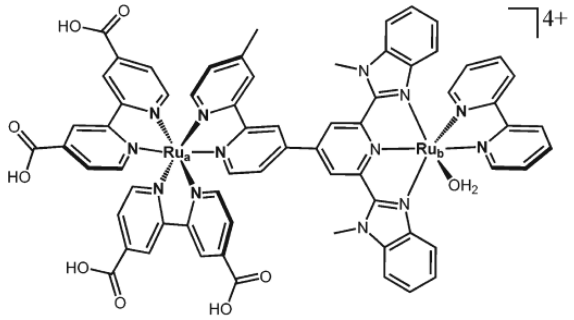

IV

When similar chromophore (Ru_a^{II}) and catalyst (Ru_b^{II}–OH_2) units were separately coadsorbed onto TiO_2 (not covalently linked), the first photo-oxidation to Ru_b^{III}–OH_2 still occurred in <20 ns, which was attributed to surface hole hopping between neighboring molecules.[30] However, preoxidized samples (Ru_b^{III}–OH_2) did not show any sign of Ru_b^{IV} species formation in laser flash experiments. Instead, the electrons injected into TiO_2 recombined with both the chromophores that had just injected (Ru_a^{III}) and with the preoxidized catalysts (Ru_b^{III}) on a time scale of 10–100 μs. Apparently, surface hole transfer to form Ru_b^{IV}=OH could not compete with recombination, which was attributed to its low driving force ($-\Delta G^{\circ\prime}$ = 0.07 eV). By taking some measures to increase the generation rate of oxidative equivalents and retard recombination, however, the authors

DOI: 10.1021/ar500386x
Acc. Chem. Res. 2015, 48, 840–850

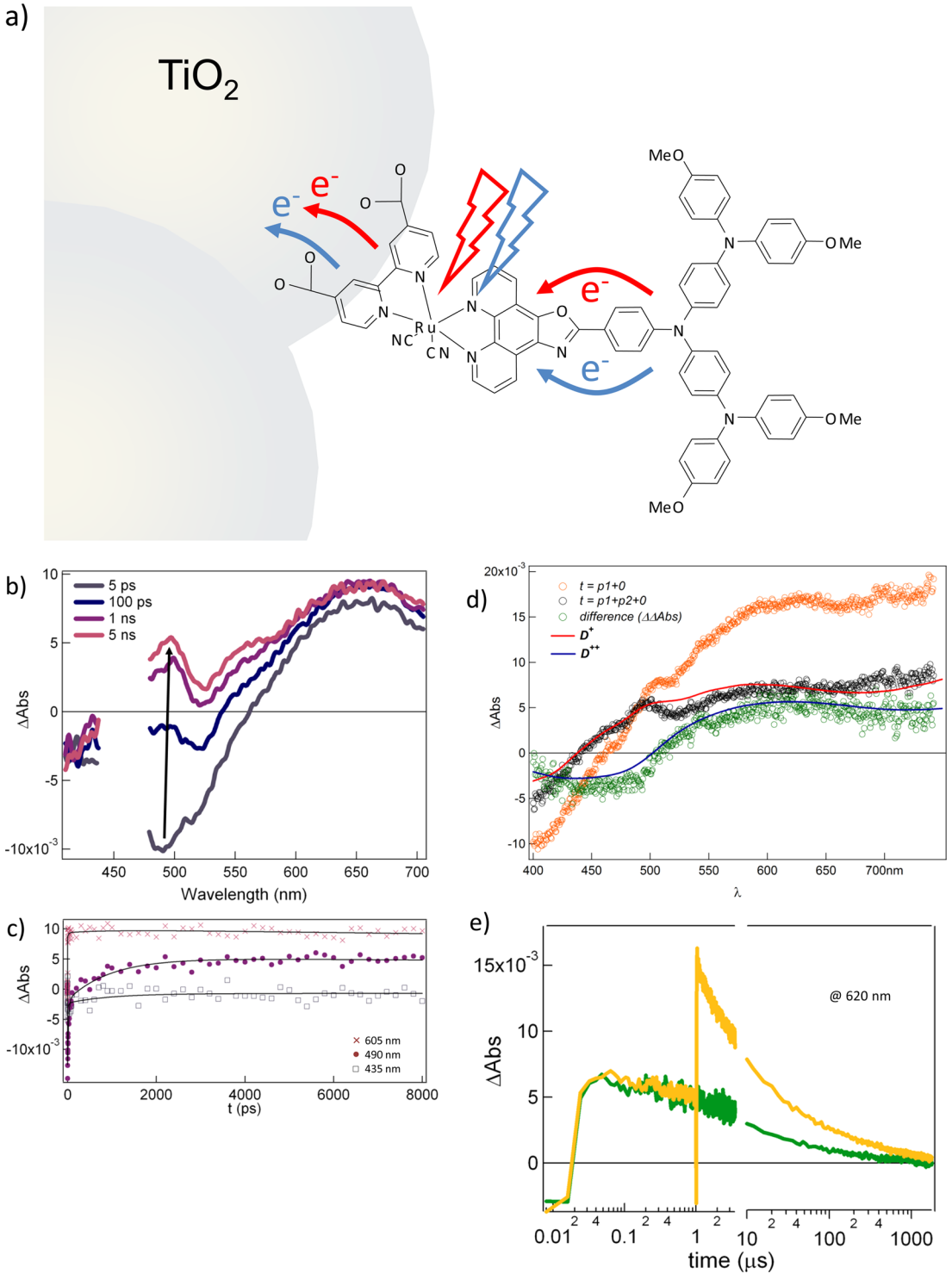

Figure 7. (a) The first molecular system to demonstrate accumulative charge separation. (b) Transient absorption spectra and (c) traces showing regeneration of the Ru^{II} sensitizer after electron injection by hole transfer to the OTA on a 30 ps to 1 ns time scale. (d) Transient absorption spectra at 100 ns after single (black) and double (orange) pulse excitation; the red line is the OTA^{+} reference spectrum. After subtraction of singly excited species signals from the orange spectrum, the remaining doubly excited spectrum (green) matches that of the OTA^{2+} reference (blue line). (e) Decay of the charge separated state after single and double pulse excitation.

could demonstrate buildup of Ru_b^{IV}═O. They used continuous irradiation to accumulate product and a larger ratio of sensitizers versus catalysts. Finally, they applied a bias on the TiO_2 electrode, to extract electrons and prevent recombination. Catalytic turnover under these conditions was not shown but indicated as a possibility.

DYE-SENSITIZED SOLAR FUEL DEVICES (DSSFDs)

The concept above extends naturally to complete devices based on dye-sensitized semiconductor electrodes coupled to molecular catalysts (Figure 8). Both the anode and cathode could be photoactive, forming a tandem device with a higher potential efficiency than for a single light-absorber system.

DOI: 10.1021/ar500386x
Acc. Chem. Res. 2015, 48, 840−850

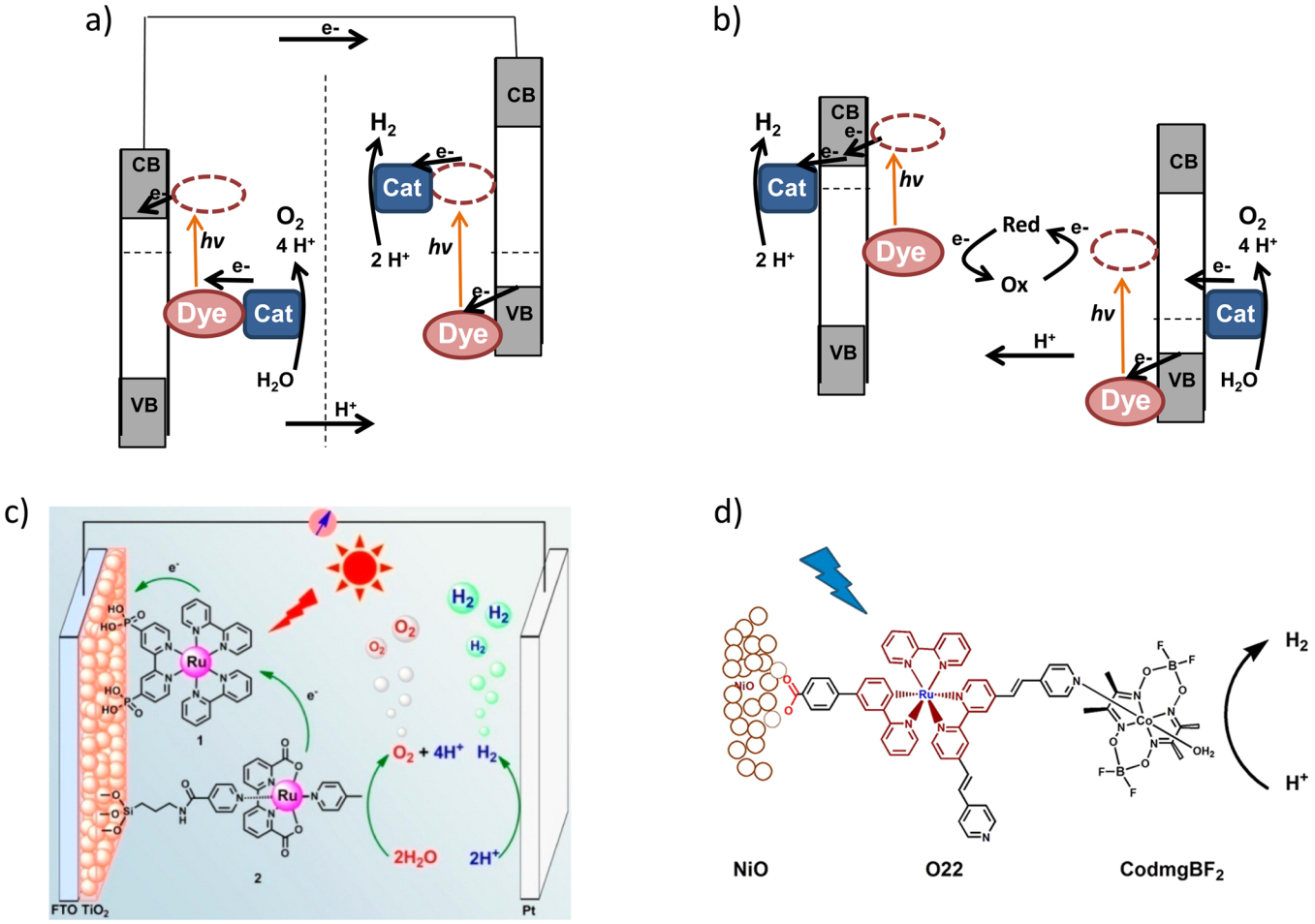

Figure 8. Schematic diagrams of a dye-sensitized solar fuel device. (a) The anode and cathode are electronically connected via an external circuit. (b) The catalysts are driven by direct coupling to the semiconductors, and a redox shuttle closes the circuit. (c, d) Examples of a dye-sensitized photoanode (from ref 32) and photocatode (from ref 33) with molecular catalysts for water oxidation and proton reduction, respectively, in aqueous media. Panels c and d are reproduced with permission from refs 32 and 33, respectively. Copyright 2013 American Chemical Society.

The semiconductors provide large internal surface area and transport of charge carriers, while molecular dyes and catalysts absorb light and couple charge separation to catalysis. The catalysts could be coupled to the sensitizers or directly to the semiconductors, which results in important differences (cf. Figure 8a,b). The electrodes of Figure 8a are connected via an external circuit, which makes compartmentalization to achieve product separation straightforward, with for example, a proton-conducting membrane to allow proton flux from anode to cathode. In Figure 8b, the electrodes are instead connected via a solution redox couple. Therefore, charge recombination of catalyst and semiconductor with the redox couple is an issue, just like for dye-sensitized solar cells (DSSCs). In Figure 8a, the critical recombination to avoid is instead that between the catalyst and semiconductor. Another difference is related to the semiconductor band energies: whereas the quasi-Fermi levels in the anode and cathode are the same in Figure 8a, they need to straddle the potentials for fuel formation and water oxidation in Figure 8b. On the other hand, the requirements on the dye redox potentials are more relaxed in the latter case.

Redox shuttle systems analogous to Figure 8b have been used for nonmolecular semiconductor systems.[31] In contrast, only a handful of molecular devices have been made based on Figure 8a, and two examples are shown in Figure 8c,d.[32,33] They have so far only involved one photoactive electrode, typically with a platinum counter electrode. They have all used a bias voltage on the photoelectrode to retard recombination and extract charges more efficiently. For a stand-alone, practical device, a bias could be provided by a coupled photovoltaic unit. Because this increases system cost, it is desirable to develop unbiased DSSFDs. The present devices show limited stability and low energy conversion efficiencies, with photocurrents of typically a few hundreds of μA cm^{-2} or lower, the highest value reported (> 2 mA cm^{-2}) being that for the system of Figure 8c. For comparison, dye-sensitized photovoltaics with close to 100% photon-to-current conversion efficiencies give current densities around 20 mA cm^{-2}.[28] These are very early devices, however, and substantial improvements can be expected in the near future.

There is yet very little mechanistic information on the devices, but based on their presumed structure and function one may make the following assumptions. First, both photoanode and photocathode materials allow for ultrafast (<1 ps) charge injection if the dye energetics and electronic coupling are sufficient.[28,34] This is a good condition to avoid reverse electron transfer and other undesirable quenching mechanisms. Second, the main bottleneck is presumably recombination of the semiconductor charge carriers with redox equivalents accumulated on the catalysts. This problem is particularly large for the photocathodes (Figure 8d), since interfacial recombination seems to be intrinsically much faster with NiO than with

DOI: 10.1021/ar500386x
Acc. Chem. Res. 2015, 48, 840−850

TiO_2.[34] Recombination may be retarded by the use of blocking layers between catalyst and semiconductor; ideally these units should not be in direct electrical contact (cf. Figure 1b). A larger dye/catalyst ratio may also focus redox equivalents on the catalysts and accelerate turnover to better compete with recombination. Third, while degradation of the molecular components is currently a problem, they may be stabilized by incorporation in a device, for example, by embedding in a matrix to provide steric protection. Promising examples of substantial catalyst stabilization upon immobilization already exist, even if the reason for this effect is not yet clear.[35,36] A convincing example is the DSSC, where the classic ruthenium dye "N3" degrades in an hour under irradiation in solution but is kinetically stabilized in the DSSC to provide an estimated lifetime of up to 20 years.[28]

CONCLUDING REMARKS

Is it possible to realize a completely molecular system based on Figure 1? Thylakoid membranes of oxygenic photosynthesis are indeed (supra)molecular systems. It should be possible to demonstrate accumulative charge separation as in Figure 7 but with TiO_2 replaced by molecular components: a rapid single-electron acceptor that is coupled to a multielectron acceptor, according to the principles outlined above. Also, for a complete photocatalytic system that couples charge separation to relatively slow catalysis, the inorganic semiconductors of Figure 8 may be replaced by organic, conducting polymers. But while molecular design allows (in principle) for precise control and tuning of properties and interactions, organic and inorganic bulk and mesoscopic materials offer alternative routes to integrated systems with molecular catalysts. Molecular−semiconductor hybrid systems may therefore take advantage of both the high design potential of molecular catalysts and the favorable charge separation properties of accessible semiconductors. Development of such systems is currently an important effort in solar fuels research.

AUTHOR INFORMATION

Corresponding Author

*E-mail: leif.hammarstrom@kemi.uu.se.

Notes

The authors declare no competing financial interest.

Biography

Leif Hammarström received his Ph.D. degree from Uppsala University in 1995. In 1996, he was a Marie-Curie Postdoctoral researcher at the University of Bologna. He was awarded an Assistant Professor position from the Swedish Research Council (1998−2001) and a Research Fellow position (2002−2007) from the Royal Academy of Sciences. Since 2004, he has been full professor of Chemical Physics at Uppsala University. He is one of the research leaders of the Swedish Consortium for Artificial Photosynthesis (CAP). His research interests include artificial photosynthesis, coupled electron transfers, photophysics, and photochemical reactions.

ACKNOWLEDGMENTS

The paper is dedicated to the Swedish Consortium for Artificial Photosynthesis (CAP) on its 20th anniversary. Financial support from the Knut and Alice Wallenberg Foundation, The Swedish Energy Agency, and The Swedish Research Council is gratefully acknowledged.

REFERENCES

(1) Balzani, V.; Credi, A.; Venturi, M. Photochemical Conversion of Solar Energy. *ChemSusChem* **2008**, *1*, 26−58.
(2) Alstrum-Acevedo, J.-H.; Brennaman, M. K.; Meyer, T. J. Chemical Approaches to Artificial Photosynthesis. 2. *Inorg. Chem.* **2005**, *44*, 6802−6827.
(3) Sun, L.; Hammarström, L.; Åkermark, B.; Styring, S. Towards Artificial Photosynthesis: Ruthenium − Manganese Chemistry for Energy Production. *Chem. Soc. Rev.* **2001**, *30*, 36−49.
(4) Wasielewski, M. R. Photoinduced Electron-Transfer in Supramolecular Systems for Artificial Photosynthesis. *Chem. Rev.* **1992**, *92*, 435−461.
(5) Gust, D.; Moore, T. A.; Moore, A. L. Molecular Mimicry of Photosynthetic Energy and Electron Transfer. *Acc. Chem. Res.* **1993**, *26*, 198−205.
(6) Eckenhoff, W. T.; Eisenberg, R. Molecular Systems for Light Driven Hydrogen Production. *Dalton Trans.* **2012**, *41*, 13004−13021.
(7) Esswein, A. J.; Nocera, D. G. Hydrogen Production by Molecular Photocatalysis. *Chem. Rev.* **2007**, *107*, 4022−4047.
(8) Artero, V.; Fontecave, M. Solar Fuels Generation and Molecular Systems: Is it Homogeneous or Heterogeneous Catalysis? *Chem. Soc. Rev.* **2013**, *42*, 2338−2356.
(9) Hammarström, L.; Sun, L.; Åkermark, B.; Styring, S. A Biomimetic Approach to Artificial Photosynthesis: Ru(II)−polypyridine Photo-Sensitisers Linked to Tyrosine and Manganese Electron Donors. *Spectrochim. Acta, Part A* **2001**, *37*, 2145−2160.
(10) Magnuson, A.; Anderlund, M.; Johansson, O.; Lindblad, P.; Lomoth, R.; Polivka, T.; Ott, S.; Stensjö, K.; Styring, S.; Sundström, V.; Hammarström, L. Biomimetic and Microbial Approaches to Solar Fuel Generation. *Acc. Chem. Res.* **2009**, *42*, 1899−1909.
(11) Evans, D. H. One-Electron and Two-Electron Transfers in Electrochemistry and Homogeneous Solution Reactions. *Chem. Rev.* **2008**, *108*, 2113−2144.
(12) Huynh, M. H. V.; Meyer, T. J. Proton-Coupled Electron Transfer. *Chem. Rev.* **2007**, *107*, 5004−5064.
(13) Hayes, R. T.; Wasielewski, M. R.; Gosztola, D. Ultrafast Photoswitched Charge Transmission through the Bridge Molecule in a Donor-Bridge-Acceptor System. *J. Am. Chem. Soc.* **2000**, *122*, 5563−5567.
(14) Lukas, A. S.; Miller, S. E.; Wasielewski, M. R. Femtosecond Optical Switching of Electron Transport Direction in Branched Donor-Acceptor Arrays. *J. Phys. Chem. B* **2000**, *104*, 931−940.
(15) Lomoth, R.; Häupl, T.; Johansson, O.; Hammarström, L. Redox-Switchable Direction of Photoinduced Electron Transfer in an $Ru(bpy)_3^{2+}$ - Viologen Dyad. *Chem.—Eur. J.* **2002**, *8*, 102−110.
(16) Xu, Y.; Eilers, G.; Borgström, M.; Pan, J.; Abrahamsson, M.; Magnuson, A.; Lomoth, R.; Bergquist, J.; Polívka, T.; Sun, L.; Sundström, V.; Styring, S.; Hammarström, L.; Åkermark, B. Synthesis and Characterization of Dinuclear Ruthenium Complexes Covalently Linked to Ru(II) tris-bipyridine: An Approach to Mimics of the Donor Side of PSII. *Chem.—Eur. J.* **2005**, *11*, 7305−7314.
(17) Flamigni, L.; Baranoff, E.; Collin, J.-P.; Sauvage, J.-P.; Ventura, B. Light Intensity Effects on Photoinduced Charge Separation Parameters in a Molecular Triad Based on an Iridium(III) bis(terpyridine) unit. *ChemPhysChem* **2007**, *8*, 1943−1949.
(18) Odobel, F.; Séverac, M.; Pellegrin, Y.; Blart, E.; Fosse, C.; Cannizzo, C.; Mayer, C. R.; Elliott, K. J.; Harriman, A. Coupled Sensitizer−Catalyst Dyads: Electron-Transfer Reactions in a Perylene−Polyoxometalate Conjugate. *Chem.—Eur. J.* **2009**, *15*, 3130−3138.
(19) Borgström, M.; Shaikh, N.; Johansson, O.; Anderlund, M. F.; Styring, S.; Åkermark, B.; Magnuson, A.; Hammarström, L. Light Induced Manganese Oxidation and Long-Lived Charge Separation in a $Mn_2^{II,II}$-$Ru^{II}(bpy)_3$-Acceptor Triad. *J. Am. Chem. Soc.* **2005**, *127*, 17504−17515.
(20) Karlsson, S. Single and Accumulative Electron Transfer − Prerequisites for Artificial Photosynthesis. PhD dissertation, Uppsala University, 2010.
(21) Eilers, G.; Lomoth, R.; Hammarström, L. Unpublished results.

DOI: 10.1021/ar500386x
Acc. Chem. Res. 2015, 48, 840−850

(22) Molnar, S. M.; Nallas, G.; Bridgewater, J. S.; Brewer, K. J. Photoinitiated Electron Collection in a Mixed-Metal Trimetallic Complex of the Form $([(bpy)_2Ru(dpb)]_2IrCl_2)(PF_6)_5$ (bpy=2,2′-bipryidine and dpb=2,3-*bis*(2-pyridyl)benzoquinoxaline). *J. Am. Chem. Soc.* **1994**, *116*, 5206−5210.
(23) Konduri, R.; Ye, H. W.; MacDonnell, F. M.; Serroni, S.; Campagna, S.; Rajeshwar, K. Ruthenium Photocatalysts Capable of Reversibly Storing up to Four Electrons in a Single Acceptor Ligand: A Step Closer to Artificial Photosynthesis. *Angew. Chem, Int. Ed.* **2002**, *41*, 3185−3188.
(24) Hammarström, L.; Styring, S. Proton-Coupled Electron Transfer of Tyrosines in Photosystem II and Model Systems for Artificial Photosynthesis: The Role of a Redox-Active Link between Catalyst and Photosensitizer. *Energy Environ. Sci.* **2011**, *4*, 2379−2388.
(25) Lubitz, W.; Reijerse, E. J.; Messinger, J. Solar Water-Splitting into H_2 and O_2: Design Principles of Photosystem II and Hydrogenases. *Energy Environ. Sci.* **2008**, *1*, 15−31.
(26) Karlsson, S.; Boixel, J.; Pelegrin, Y.; Blart, E.; Becker, H.-C.; Odobel, F.; Hammarström, L. Accumulative Charge Separation Inspired by Photosynthesis. *J. Am. Chem. Soc.* **2010**, *132*, 17977−17979.
(27) Karlsson, S.; Boixel, J.; Pelegrin, Y.; Blart, E.; Becker, H.-C.; Odobel, F.; Hammarström, L. Accumulative Electron Transfer: Multiple Charge Separation in Artificial Photosynthesis. *Faraday Disc.* **2012**, *155*, 233−252.
(28) Hagfeldt, A.; Boschloo, G.; Sun, L.; Kloo, L.; Pettersson, H. Dye-Sensitized Solar Cells. *Chem. Rev.* **2010**, *110*, 6595−6663.
(29) Song, W.; Glasson, C. R. K.; Luo, H.; Hanson, K.; Brennaman, M. K.; Concepcion, J. J.; Meyer, T. J. Photoinduced Stepwise Oxidative Activation of a Chromophore-Catalyst Assembly on TiO_2. *J. Phys. Chem. Lett.* **2011**, *2*, 1808−1813.
(30) Song, W.; Ito, A.; Binstead, R. A.; Hanson, K.; Luo, H.; Brennaman, M. K.; Concepcion, J. J.; Meyer, T. J. Accumulation of Multiple Oxidative Equivalents at a Single Site by Cross-Surface Electron Transfer on TiO_2. *J. Am. Chem. Soc.* **2013**, *135*, 11587−11594.
(31) Kudo, A.; Miseki, Y. Heterogeneous Photocatalyst Materials for Water Splitting. *Chem. Soc. Rev.* **2009**, *38*, 253−278.
(32) Gao, Y.; Ding, X.; Liu, J.; Wang, L.; Lu, Z.; Li, L.; Sun, L. Visible Light Driven Water Splitting in a Molecular Device with Unprecedentedly High Photocurrent Density. *J. Am. Chem. Soc.* **2013**, *135*, 4219−4222.
(33) Ji, Z.; He, M.; Huang, Z.; Ozkan, U.; Wu, Y. Photostable p-Type Dye-Sensitized Photoelectrochemical Cells for Water Reduction. *J. Am. Chem. Soc.* **2013**, *135*, 11696−11699.
(34) Odobel, F.; Pellegrin, Y.; Gibson, E. A.; Hagfeldt, A.; Smeigh, A. L.; Hammarström, L. Recent Advances and Future Directions to Optimize the Performance of p-Type Dye-Sensitized Solar Cells. *Coord. Chem. Rev.* **2012**, *256*, 2414−2423.
(35) Andreiadis, E. S.; Jacques, P.-A.; Tran, P. D.; Leyris, A.; Chavarot-Kerlidou, M.; Jousselme, B.; Matheron, M.; Pecaut, J.; Palacin, S.; Fontecave, M.; Artero, V. Molecular Engineering of a Cobalt-Based Electrocatalytic Nanomaterial for H_2 Evolution under Fully Aqueous Conditions. *Nat. Chem.* **2013**, *4*, 48−53.
(36) Pullen, S.; Fei, H.; Orthaber, A.; Cohen, S. M.; Ott, S. Enhanced Photochemical Hydrogen Production by a Molecular Diiron Catalyst Incorporated into a Metal−Organic Framework. *J. Am. Chem. Soc.* **2013**, *135*, 16997−17003.

DOI: 10.1021/ar500386x
Acc. Chem. Res. 2015, 48, 840−850